

121 m would produce beaches at 216 m altitude if fully uplifted ( $1,000 \times$  (ice density) (mantle density) =  $337 \text{ m} - 121 \text{ m} = 216 \text{ m}$ ). Second, the values generally exceed the geological evidence for increased ice thickness.

The radiocarbon dates used in Andrews' method are minimum values which provide maximum values for the residual uplift. The estimated ice thicknesses are clearly too low as the geological record indicates thicker ice on the inner shelf. This suggests a longer response time in Antarctica than in Canada for isostatic equilibrium to be established after deglaciation.

Although the extent and thickness of LGM ice on the continental shelf of Antarctica cannot yet be fully assessed most geological evidence indicates that it is unlikely to have reached the shelf edge throughout its periphery. An average thickness of 500 m and a grounding line advance of 30 km over the inner shelf seem to be reasonable estimates.

If we use these figures for ice increase in the coastal zone, together with an inland decrease in thickness to 0 m at the 2,000-m contour and a sea level fall of 120 m, we can estimate LGM increase in Antarctic ice volume and its probable contribution to sea-level fall. Integrated around the 9,100-km margin of East Antarctica between  $170^\circ \text{ E}$  and  $30^\circ \text{ W}$  (excluding Lambert Glacier), this accounts for a sea-level fall of 0.73 m (calculated as  $32 \text{ km}^2 \times 9,100 \text{ km} \times 0.9$  ( $900 \text{ kg m}^{-1}$ ) divided by the world sea-level area in  $\text{km}^2$ ). The Lambert Glacier system contributed a fall of 0.13 m (assuming that the drainage area of  $2.5 \times 10^5 \text{ km}^2$  below 2,000 m increased by 200 m) to give a total fall of 0.86 m due to LGM expansion of the Southern Ocean margin of the East Antarctic ice sheet. But ice-core studies<sup>13,15</sup> indicate that the ice-sheet interior was 200–300 m lower. An average lowering of 150 m over the  $4 \times 10^6 \text{ km}^2$  area of ice sheet above 2,000 m would add 1.5 m to sea level. Thus the net effect could have raised the sea level by 0.64 m. The full contribution of Antarctica to LGM sea level fall can be estimated similarly. Reconstruction for Ross Embayment<sup>8</sup> indicates a contribution of  $\sim 0.3\text{--}0.45 \text{ m}$  lowering. The slightly larger Weddell Embayment contributed  $\sim 0.35\text{--}0.55 \text{ m}$ . The remainder of the continent, including marginal West Antarctica and the Antarctic Peninsula, contributed 0.48 m. Our estimate for Antarctica's contribution to LGM sea-level fall is thus 0.5–2.5 m.

This is less than the 25 m of the CLIMAP and other models<sup>3,25,26</sup>. As the figure of 120 m for LGM sea-level fall seems well constrained<sup>23</sup>, our interpretation does not support these models and suggests either that the estimated fall of 120 m needs reconsideration, or that Northern Hemisphere ice sheets had greater volumes than previously calculated.

These data also allow the deglacial history of Antarctica to be broadly constrained. The East Antarctic ice-sheet margin had attained its present configuration by at least 8.5–9.0 kyr BP, and probably before 10 kyr BP<sup>12,23</sup>. In Ross Embayment, the western margin of the Ross ice shelf was within 25 km of its present position by 7.2 kyr BP. In McMurdo Sound, the present coast was established before 6.6 kyr BP<sup>28</sup>, and outlet glaciers on the Transantarctic Mountains were at their current elevations by 6 kyr BP<sup>29</sup>.

Inputs to current models of sea-level change include data on the location, volume and melting histories of the LGM ice sheets<sup>25,26</sup>. These models use the CLIMAP reconstruction of the Antarctic ice sheets to derive contributions to post-glacial sea-level rise of 25 m between 9 and 4 kyr BP<sup>25</sup> and 37 m between 18 and 6 kyr BP<sup>26</sup>. Such estimates conflict with the geological data, suggesting that the models must be re-examined. This is important as the models are widely used to assess present patterns of sea-level change<sup>29,30</sup>. □

4. Drewry, D. J. *J. Glaciol.* **34**, 231–244 (1979).
5. Mayewski, P. A. & Goldthwait, R. P. *Antarct. Res. Series* **36**, 275–324 (1985).
6. Mabin, M. C. G. *South Afr. J. Sci.* **82**, 506–508 (1986).
7. Kirk, R. M. in *Quat. Research in Australian Antarctica Future Directions, Sp. Publ. 3*, 85–105 (Department of Geography and Oceanography, ADFA, Canberra, 1991).
8. Denton, G. H., Bockheim, J. C., Wilson, S. C. & Stuiver, M. *Quat. Res.* **31**, 151–182 (1989).
9. Goodwin, I. D. *Quat. Res.* (in the press).
10. Bolshiyakov, D., Verkulich, S., Pushina, Z. & Kirienko, E. in *Abstr. 6th Int. Symp. Antarctic Earth Sciences* (National Institute Polar Research, Japan, 1991).
11. Colhoun, E. A. *Polar Record* **27**, 345–355 (1991).
12. Omoto, K. *Science Reports Tohoku University 7th Series (Geography)* **27(2)**, 95–148 (1977).
13. Robin, G. de Q. *Nature* **316**, 578–579 (1985).
14. Lorius, C., Raynaud, D., Petit, J. R., Jouzel, J. & Merlivat, L. *Ann. Glaciol.* **5**, 88–94 (1984).
15. Jouzel, J. et al. *Quat. Res.* **31**, 135–150 (1989).
16. Grootes, P. M. & Stuiver, M. *Int. Assoc. Hydrol. Sci.* **170**, 269–282 (1987).
17. Barrett, P. J. (ed.) *N.Z. D.S.I.R. Bull.* **245** (Wellington, 1989).
18. Hambrey, M. J. et al. *Polar Record* **25**, 99–106 (1989).
19. Domack, E. W., Jull, A. J. T., Anderson, J. B. & Linick, T. in *Geological Evolution of Antarctica*, 693–698 (Cambridge Univ. Press 1991).
20. Adamson, D. A. & Colhoun, E. A. *Antarct. Sci.* (in the press).
21. Adamson, D. A. & Pickard, J. in *Antarctic Oasis* (Pickard, J.) 63–97 (Academic, Sydney, 1986).
22. Clark, J. A. & Lingle, C. S. *Quat. Res.* **11**, 279–298 (1978).
23. Fairbanks, R. G. *Nature* **342**, 637–642 (1989).
24. Andrews, J. T. *Can. J. Earth Sci.* **5**, 39–47 (1968).
25. Tushingham, A. M. & Peltier, W. R. *J. geophys. Res.* **96**, 4497–4523 (1991).
26. Nakada, M. & Lambeck, K. *Nature* **333**, 36–40 (1988).
27. Colhoun, E. A. & Adamson, D. A. *ANARE Res. Rep. No. 136* (Dassett, Canberra, 1992).
28. Behrendt, J. C. & Cooper, A. *Geology* **19**, 315–319 (1991).
29. Peltier, W. R. & Tushingham, A. M. *Science* **244**, 806–810 (1989).
30. Lambeck, K. *Palaeogeogr. Palaeoclim. Palaeoecol.* **89**, 205–217 (1990).
31. Drewry, D. J. *Glaciological and Geophysical Folio* (Scott Polar Research Institute, Cambridge, 1983).
32. Chinn, T. J. H., Whitehouse, I. E. & Hoefle, H. C. *Geol. Jb.* **E38**, 299–319 (1989).
33. Baroni, C. & Orbelli, G. *Quat. Res.* **36**, 157–177 (1991).
34. Speir, T. W. & Cowling, J. C. *Polar Biol.* **2**, 199–205 (1984).
35. Nichols, R. J. *J. Glaciol.* **7**, 449–478 (1968).
36. Cameron, R. L. *Am. geophys. Un. Antarct. Res. Series* **2**, 1–36 (1964).
37. Zhang, Q. & Peterson, J. A. *ANARE Res. Rep. No. 133* (1984).

## Correlation between isotope records in marine and continental carbon reservoirs near the Palaeocene/Eocene boundary

Paul L. Koch\*, James C. Zachos†  
& Philip D. Gingerich†

\* Geophysical Laboratory, Carnegie Institution of Washington, Washington DC 20015, USA

† Department of Geological Sciences, The University of Michigan, Ann Arbor, Michigan 48109, USA

CHANGES in the isotope content of the large marine carbon reservoir can force shifts in that of the smaller carbon pools in the atmosphere and on land. The carbon isotope compositions of marine carbonate sediments from the late Palaeocene vary considerably, exhibiting a sudden decrease close to the Palaeocene/Eocene boundary which coincides with deep-sea benthic extinctions<sup>1</sup> and with changes in ocean circulation. Here we report that these fluctuations in the marine carbon isotope record are closely tracked by the terrestrial records provided by palaeosol carbonates and mammalian tooth enamel. In using palaeosol carbonates to reconstruct the  $\text{CO}_2$  content of the ancient atmosphere<sup>2</sup>, isotope shifts of this sort will have to be taken into account. The sharp decrease in  $^{13}\text{C}/^{12}\text{C}$  ratios in the late Palaeocene provides a datum for precise correlation of marine and continental records, and suggests that abrupt climate warming at this time may have played an important role in the evolution of land mammals.

From the late Palaeocene ( $\sim 60$  million years ago [Myr]) to the early Eocene ( $\sim 55$  Myr)<sup>3</sup>, the carbon isotope composition of biogenic marine carbonate decreased by 3‰ (ref. 4; Fig. 1). Superimposed on this trend is a short-term drop of 2.5–4.5‰, recorded in planktonic and benthic foraminifera from the latest Palaeocene ( $\sim 57.3$  Myr)<sup>1</sup>. This unusual drop coincided with marine warming, a decrease in the surface-to-bottom water thermal gradient and mass extinction of benthic foraminifera<sup>5,6</sup>.

Received 6 January; accepted 5 June 1992.

1. Voronov, P. S. *Inform. Bull. Soc. Antarct. Expedition* **23**, 15–19 (1960).
2. Hollin, J. T. *J. Glaciol.* **4**, 173–195 (1962).
3. Stuiver, M., Denton, G. H., Hughes, T. J. & Fastook, J. L. in *The Last Great Ice Sheets* (eds Denton, G. H. & Hughes, T. J.) 319–436 (Wiley, New York, 1981).

Currently this short-term carbon excursion has only been documented at Ocean Drilling Project (ODP) site 690, but it has been reported in the equatorial Pacific<sup>7</sup>, northern Atlantic<sup>7</sup>, southern Atlantic<sup>8</sup> and Indian oceans<sup>8,9</sup> and was most probably a global marine event. Because most carbon in the Earth's biosphere, atmosphere and hydrosphere is in the oceans<sup>10</sup>, the global fluctuations in marine isotopes in the Palaeocene/Eocene should have affected atmospheric and continental carbon reservoirs. Coupling of isotope signals between Permian marine carbonates and land vertebrate hydroxyapatite has been detected previously<sup>11</sup>. We explore isotope coupling between marine carbonate and continental tooth apatite and palaeosol carbonate across the Palaeocene/Eocene boundary.

The isotope relationships between marine, atmospheric and continental carbon reservoirs are presented in Fig. 2. Atmospheric CO<sub>2</sub> is in long-term carbon isotope equilibrium with

TABLE 1 Measured  $\delta^{13}\text{C}$  for each sampling horizon in Fort Union and Willwood formations

Level	Age (Myr)	$\delta^{13}\text{C}$ (‰) EA	$\delta^{13}\text{C}$ (‰) PC	$\Delta$ (‰) PC-EA
Eocene				
2,210	55.90	-12.2	-10.1	2.1
2,110	56.10	-12.0	-8.6	3.4
2,085	56.15	-12.9		
2,050	56.20	-11.6		
2,020	56.30	-12.2		
1,995	56.35	-11.1		
1,970	56.40	-12.4	-9.0	3.4
1,935	56.45	-11.4		
1,910	56.50	-12.3	-7.9	4.4
1,870	56.60	-12.2		
1,840	56.65	-11.4	-7.4	4.0
1,760	56.80	-12.0	-8.2	3.8
1,700	56.95	-11.5	-9.1	2.4
Palaeocene				
1,665	57.00	-12.4		
1,630	57.10	-11.4	-8.2	3.2
1,570	57.20	-11.3	-8.5	2.8
1,530	57.30	-13.9		
1,525	57.30	-12.3	-9.9	2.4
1,520	57.30	-15.7	-14.5	1.2
1,515	57.30	-12.0		
1,505	57.35	-9.8		
1,495	57.35	-9.7	-11.4	-1.7
1,460	57.45	-10.9		
1,425	57.55	-11.8		
1,385	57.70	-10.4		
1,355	57.75	-11.0	-8.0	3.0
1,330	57.85	-11.2		
1,280	58.00	-9.5	-6.6	2.9
1,250	58.05	-13.2		
1,210	58.20	-9.1	-8.5	0.6
1,150	58.35	-11.2		
1,110	58.45	-11.0		
1,080	58.55	-10.1	-7.4	2.7
1,050	58.65	-9.0	-8.2	0.8
1,015	58.75	-10.7	-7.0	3.7
940	58.95	-9.9	-8.3	1.6
860	59.15	-7.0		
760	59.45	-7.4	-6.6	0.8
720	59.55	-11.0		
700	59.60	-8.7	-7.6	1.1
680	59.65	-10.5		
550	60.00	-9.2		

EA, herbivore tooth enamel apatite; PC, palaeosol carbonate; difference between these materials,  $\Delta_{\text{PC-EA}} = \delta^{13}\text{C}_{\text{PC}} - \delta^{13}\text{C}_{\text{EA}}$ . Level refers to metres above K/T boundary on Polecat Bench, Bighorn Basin, Wyoming. Ages calculated at 50,000-year intervals by linear interpolation using dates from Fig. 3.

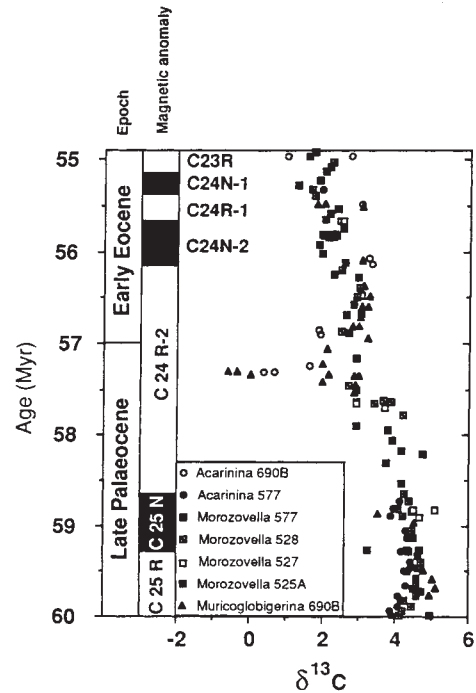


FIG. 1 Fluctuations in  $\delta^{13}\text{C}$  of near-surface planktonic foraminifera from marine waters across the Palaeocene/Eocene boundary. Note the gradual decrease from 60 Myr to 55 Myr, and the brief (<50,000 year) negative excursion at 57.3 Myr. The data are compiled from ODP holes 690B (Weddell Sea, Antarctica)<sup>30</sup>, 525A, 527 and 528 (Walvis Ridge, south Atlantic)<sup>31</sup>, and 577 (Shatsky Rise, south Pacific)<sup>32</sup>. Absolute ages follow Aubry *et al.*<sup>3</sup>, but age assignments will be shifted ~2 Myr younger by impending revisions of Palaeogene dating and stratigraphy (C. Swisher, personal communication)<sup>27</sup>.  $\delta^{13}\text{C} = [({}^{13}\text{C}/{}^{12}\text{C})_{\text{sample}} / ({}^{13}\text{C}/{}^{12}\text{C})_{\text{standard}} - 1]$ , where standard is PDB.

calcium carbonate in the tests of surficial marine organisms, with a temperature-dependent offset of ~9‰ (ref. 12). These carbon reservoirs may decouple transiently, but equilibration should occur rapidly because of the high rates of marine carbon turnover (<5,000 years) and exchange between the ocean mixed layer and the atmosphere (<50 years)<sup>10</sup>.

As land plants fix atmospheric CO<sub>2</sub> by photosynthesis, they fractionate carbon isotopes, preferentially incorporating <sup>12</sup>C. Although different photosynthetic pathways (C3, C4 or CAM) exist today, Palaeocene/Eocene floras were dominated by C3 plants<sup>13,14</sup>. Modern C3 plants and atmospheric CO<sub>2</sub> differ by -19.5 ± 2‰ (ref. 15). Vertebrate herbivores eat plants, and deposit carbonate hydroxyapatite in their teeth that differs in <sup>13</sup>C content ( $\delta^{13}\text{C}$ ; see Fig. 1) from their diets by +12 ± 1‰ (ref. 16). Thus land plants and herbivores track changes in the  $\delta^{13}\text{C}$  of atmospheric CO<sub>2</sub> that are ultimately driven by the ocean.

The CO<sub>2</sub> gas deep in a soil is supplied by decay of plants and root respiration, which produce CO<sub>2</sub> that is isotopically similar to source plants<sup>17</sup>. Atmospheric CO<sub>2</sub>, which has a less negative  $\delta^{13}\text{C}$  than plants, mixes into soils, impeding the outward diffusion of soil CO<sub>2</sub>. Consequently, the  $\delta^{13}\text{C}$  of soil CO<sub>2</sub> is higher than purely plant-derived CO<sub>2</sub> (ref. 18). Below ~30 cm, soil CO<sub>2</sub> is isotopically homogeneous, and soil carbonates from these depths, which form in isotopic equilibrium with soil CO<sub>2</sub>, have  $\delta^{13}\text{C}$  values ~15‰ greater than the overlying flora<sup>17,19</sup>. Model experiments have shown, however, that if the atmospheric concentration of CO<sub>2</sub> (*p*CO<sub>2</sub>) was higher in the past, atmospheric penetration into soils would be greater, increasing both the  $\delta^{13}\text{C}$  of soil carbonates and the difference in  $\delta^{13}\text{C}$  between carbonate and plants<sup>2</sup>. These model results have been developed into a method for estimating *p*CO<sub>2</sub> using the  $\delta^{13}\text{C}$  of palaeosol carbonate<sup>2,20</sup>.

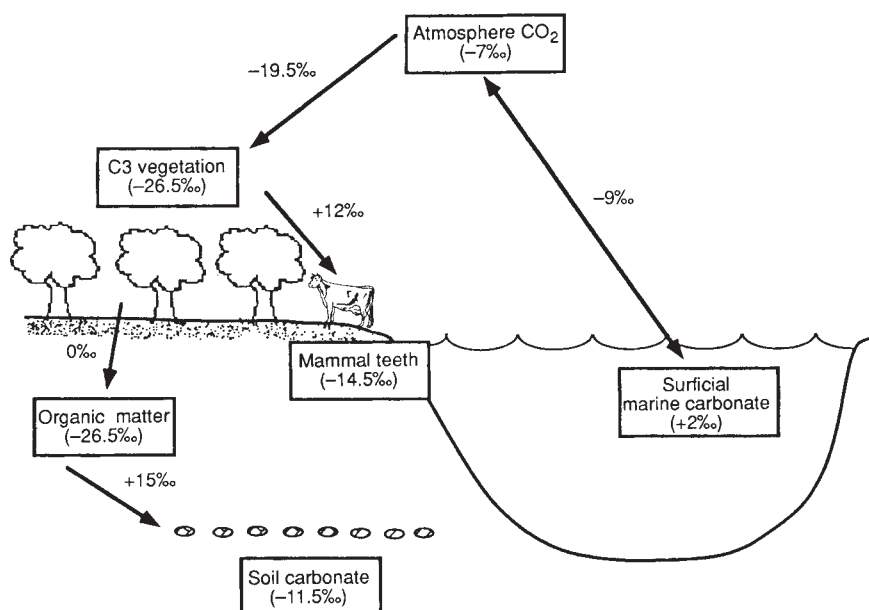


FIG. 2 Model of coupling between marine, atmospheric and continental carbon reservoirs. Equilibrium fractionation between surficial marine carbonate and atmospheric CO<sub>2</sub> is  $\sim -9\%$  when temperatures range from 20–30 °C (ref. 12). The model assumes that Palaeocene/Eocene floras had only C3 plants; the fractionation characteristic of these plants ( $-19.5\%$ ) was used<sup>15</sup>. The modern value for the difference between plants and soil carbonate was used (15%), but this value would increase if atmospheric  $p_{\text{CO}_2}$  was greater than its present value<sup>2</sup>. Palaeosol carbonate  $\delta^{13}\text{C}$  are  $\sim 3\%$  greater than enamel apatite  $\delta^{13}\text{C}$ , but this difference would also increase if  $p_{\text{CO}_2}$  were higher. Typical values for modern C3 ecosystems are supplied in boxes.

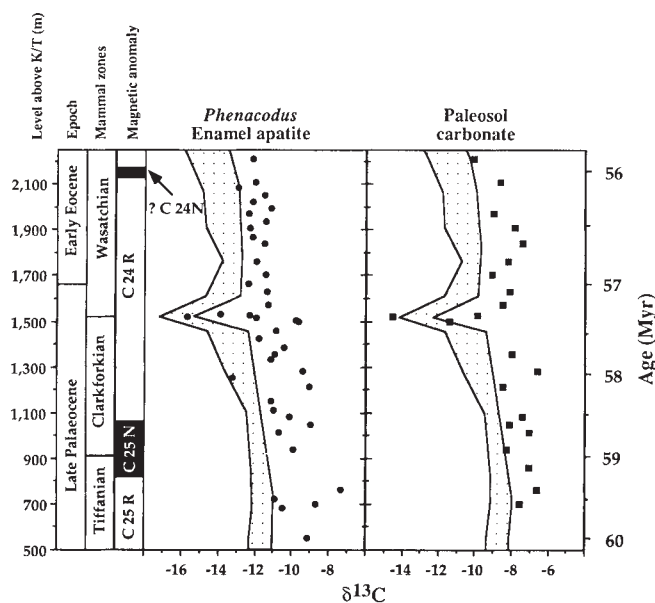


FIG. 3 Trends in  $\delta^{13}\text{C}$  across the Palaeocene/Eocene boundary in the Bighorn Basin, Wyoming; points are from enamel apatite and palaeosol carbonate, shaded regions are values predicted from biogenic marine carbonate. Predicted values were calculated at 500,000-year intervals using the high and low  $\delta^{13}\text{C}$  values for marine carbonates from Fig. 1. We first calculated a range of  $\delta^{13}\text{C}$  values for atmospheric CO<sub>2</sub>, assuming equilibrium fractionation with high and low  $\delta^{13}\text{C}$  values for marine carbonate at 20 and 30 °C. We then applied values from Fig. 2 for fractionations between atmosphere, plants, enamel apatite and palaeosol carbonate, and plotted the maximum calculated range for each interval. Level refers to metres above the K/T boundary in the Clarks Fork region<sup>21,22</sup>. Marine and continental correlation and ages were determined using four points, including the bottom of C25R at 60.2 Myr, the bottom of C24R-2 at 58.6, and the age of 57.3 for carbon isotope excursions. The fourth point was an age of 55.9 Myr for the base of Wa5, which was correlated using mammalian biostratigraphy to the southern Bighorn Basin. An age for this level in the southern Bighorn Basin was obtained by linear interpolation between an <sup>40</sup>Ar–<sup>39</sup>Ar dated level in the upper Wasatchian, and a date for a level in the Clarkforkian supplied by palynofloral correlation to the marine NP9/NP10 boundary<sup>27</sup>.

We sought evidence of isotope coupling between the oceans and continents by analysing mammal teeth and palaeosol carbonates from the continental Fort Union and Willwood formations in the Bighorn Basin, northwestern Wyoming, which provide a continuous sequence spanning the Palaeocene/Eocene boundary (Fig. 3)<sup>21,22</sup>. Tooth enamel was collected from the herbivorous mammal, *Phenacodus*, then treated with NaOCl and dilute acetic acid to remove organic matter and diagenetic carbonates<sup>23</sup>. Unlike bone apatite, which is highly susceptible to post-mortem alteration, enamel apatite is resistant, owing to its greater crystal size and lower porosity<sup>23,24</sup>. Palaeosols occurred as thin, organic-rich A horizons (when present) overlying thicker yellow, red, orange or purple B horizons<sup>25</sup>. We collected micritic carbonate nodules from  $\geq 30$  cm below original palaeosol surfaces, and isotope samples from nonrecrystallized zones in nodules. Samples were analysed on a Finnigan MAT 251 mass spectrometer linked to a Kiel automatic carbonate preparation device. Carbonate and apatite were reacted at 75 °C for 5 and 15 minutes, respectively. Samples were calibrated to PDB using NBS 20, with a precision of  $\leq 0.1\%$ .

The gradual decrease in marine  $\delta^{13}\text{C}$  from late Palaeocene

(60 Myr) to early Eocene (56 Myr) was closely tracked by enamel apatite and palaeosol carbonate. The  $\delta^{13}\text{C}$  of palaeosol carbonate decreased from  $-7$  to  $-10\%$ , whereas enamel apatite dropped from  $-8$  to  $-12\%$  (Table 1, Fig. 3). Peak values for land and marine  $\delta^{13}\text{C}$  occurred within C25R, and values for both records decreased through C25N and C24R (Figs 1 and 3).

Continental materials also record an extraordinary drop precisely at the Clarkforkian/Wasatchian (Cf/Wa) boundary (Fig. 3). The  $\delta^{13}\text{C}$  of enamel apatite and palaeosol carbonate dropped by 5.9 and 4.5%, respectively, in less than 50,000 years; these low values persisted for less than 100,000 years (Fig. 3). This continental carbon isotope excursion was very similar to the latest Palaeocene marine carbon excursion in magnitude, direction and duration (Figs 1 and 3, ref. 1). When the marine and continental records are correlated, using magnetostratigraphy<sup>3,21</sup>, palynoflora and radiometric dates<sup>26,27</sup> (Fig. 3), estimates for the age of the marine and continental excursions differ by only 150,000 years. This apparent age difference is remarkably small, particularly when compared with the uncertainties for the ages of the isochrons used to correlate continental and marine strata. Given their strong similarities in timing and

character, we conclude that the latest Palaeocene marine excursion in isotope ratios and the continental excursion at the Cf/Wa boundary were isochronous.

Differences in  $\delta^{13}\text{C}$  between palaeosol carbonate and enamel apatite were similar to differences between these components today (Table 1). Furthermore, palaeosol carbonate and enamel apatite had  $\delta^{13}\text{C}$  values close to those predicted from marine carbonate (Fig. 3). The persistent 1–2‰ offset between predicted and observed values is puzzling. A diagenetic explanation is unlikely, because it would entail identical alteration of two different minerals, apatite and calcite, to maintain the appropriate isotope spacing observed between the minerals. A small fraction of C4 plants in the Palaeocene/Eocene could explain the offset. This idea is not supported by most palaeobotanical or isotope evidence from fossil organic matter<sup>13,14</sup>, although the possibility of non-C3 plants before the Miocene is controversial<sup>28</sup>. We attribute the offset to uncertainties in values for model parameters, particularly for ocean-atmosphere and atmosphere-plant fractionations. Atmosphere-plant fractionation, for example, covaries with temperature, light intensity and  $p_{\text{CO}_2}$  (ref. 15), all of which may have been different in the Palaeocene/Eocene. Given these possible sources of error, the model and observed records are remarkably similar.

Coupling of marine and continental carbon reservoirs has three important implications. To determine ancient  $p_{\text{CO}_2}$  using palaeosol carbonates, the  $\delta^{13}\text{C}$  of ancient C3 plants and atmospheric  $\text{CO}_2$  must be estimated. In past applications of the method, it was argued that these carbon reservoirs were isotopically constant through geological time<sup>2,20</sup>. We have demonstrated, however, that the  $\delta^{13}\text{C}$  of C3 plants and atmospheric  $\text{CO}_2$  can vary substantially; thus they must be independently monitored. We used Cerling's model<sup>2</sup> to recalculate Palaeocene/Eocene atmospheric  $p_{\text{CO}_2}$ , but estimated the  $\delta^{13}\text{C}$  of C3 plants and atmospheric  $\text{CO}_2$  using enamel apatite. Throughout the entire interval, including the excursion at the Cf/Wa boundary, we calculated  $p_{\text{CO}_2}$  values of  $\leq 350$  p.p.m.v., lower than Cerling's result ( $< 750$  p.p.m.v.), calculated assuming modern  $\delta^{13}\text{C}$  for C3 plants and atmospheric  $\text{CO}_2$ . Yet both studies indicated relatively low  $p_{\text{CO}_2}$  values (1–2 times modern levels) at this time, consistent with independent estimates from modelling experiments<sup>29</sup>.

The sharp, isochronous, global drop in  $\delta^{13}\text{C}$  provides a datum linking the marine and continental realms near the Palaeocene/Eocene boundary, an interval of considerable stratigraphic controversy<sup>3,21,26,27</sup>. The marine isotope excursion and the benthic extinction immediately precede the marine Palaeocene/Eocene boundary<sup>1,3,4</sup>, which lies within calcareous nannoplankton zone NP10 and within planktonic foraminiferal zone P6b. On land, the isotope excursion marks the Cf/Wa boundary. Thus the currently defined marine Palaeocene/Eocene boundary corresponds to a level within the earliest Wasatchian land mammal age.

The carbon isotope excursion links the sudden extinction of deep sea organisms with the onset of evolutionary changes in late Palaeocene land mammals, including the first appearance of important groups such as artiodactyls, perissodactyls and primates<sup>22</sup>. The benthic extinction has been attributed to sudden change in ocean circulation, possibly resulting in deep-sea warming<sup>1,6</sup>. Perhaps abrupt climate warming spurred morphological changes in mammals, or perhaps the brief period (~100,000 years) of warmth in high latitudes permitted dispersal of new forms between continents. The marine-continental linkage provided by carbon isotopes indicates a more prominent role for climate warming in the evolution of Palaeocene land mammals than was previously realized. □

- Shackleton, N. J. *Palaeogeogr. Palaeoclim. Palaeoecol.* **57**, 91–102 (1986).
- Tjalsma, R. C. & Lohmann, G. P. *Micropaleont. spec. Publ.* 4 (Micropaleontology Press, New York, 1983).
- Thomas, E. *Proc. Ocean Drilling Prog. B* **113**, 571–594 (1990).
- Pak, D. K., Miller, K. G. & Wright, J. D. *Geol. Soc. Am. Abstr. A* **141** (1991).
- Thomas, E. *Geol. Soc. Am. Abstr.* **23**(5), A141 (1991).
- Barrera, E. *Geol. Soc. Am. Abstr.* **23**(5), A179 (1991).
- Sundquist, E. T. in *The Carbon Cycle and Atmospheric  $\text{CO}_2$ : Natural Variations Archaean to Present* (eds Sundquist, E. T. & Broecker, W. S.) 5–59 (American Geophysical Union, 1985).
- Thackeray, J. F. *et al. Nature* **347**, 751–753 (1990).
- Mook, W. G. *Neth. J. Sea Res.* **20**, 211–223 (1986).
- Popp, B. N., Takigiku, R., Hayes, J. M., Louda, J. W. & Baker, E. W. *Am. J. Sci.* **289**, 436–454 (1989).
- Raven, J. A. & Sprent, J. I. *J. geol. Soc. Lond.* **146**, 161–170 (1989).
- O'Leary, M. H. *Bioscience* **38**, 328–336 (1988).
- Lee-Thorp, J. A., Sealy, J. C. & van der Merwe, N. J. *J. archaeol. Sci.* **16**, 585–599 (1989).
- Quade, J. A., Cerling, T. E. & Bowman, J. R. *Geol. Soc. Am. Bull.* **101**, 464–475 (1989).
- Cerling, T. E., Solomon, D. K., Quade, J. & Bowman, J. R. *Geochim. cosmochim. Acta* **55**, 3403–3405 (1991).
- Cerling, T. E., Quade, J. A., Wang, Y. & Bowman, J. R. *Nature* **341**, 138–139 (1989).
- Mora, C. I., Driese, S. G. & Seager, P. G. *Geology* **19**, 1017–1020 (1991).
- Butler, R. F., Gingerich, P. D. & Lindsay, E. H. *J. Geol.* **89**, 299–316 (1981).
- Gingerich, P. D. *Univ. Mich. Papers Paleontol.* **28**, 1–97 (1989).
- Lee-Thorp, J. A. & van der Merwe, N. J. *J. archaeol. Sci.* **19**, 343–354 (1991).
- Lee-Thorp, J. A. & van der Merwe, N. J. *S. Afr. J. Sci.* **83**, 71–74 (1987).
- Bown, T. M. & Kraus, M. J. *Palaeogeogr. Palaeoclim. Palaeoecol.* **34**, 1–30 (1981).
- Wing, S. L. *Science* **226**, 439–441 (1984).
- Wing, S. L., Bown, T. M. & Obradovich, J. D. *Geology* **19**, 1189–1192 (1991).
- Wright, V. P. & Vanstone, S. D. *J. geol. Soc. Lond.* **148**, 945–947 (1991).
- Berner, R. A. *Am. J. Sci.* **291**, 339–376 (1989).
- Stott, L. D., Kennett, J. P., Shackleton, N. J. & Corfield, R. M. *Proc. ODP Scient. Results* **113** (eds Barker, P. F. *et al.*) 849–863 (Ocean Drilling Program, College Station, Texas, 1990).
- Shackleton, N. J., Hall, M. A. & Boersma, A. *Init. Rep. DSDP* **74** (eds Moore, T. C. *et al.*) 599–612 (U.S. Government Printing Office, Washington DC, 1984).
- Corfield, R. M., Cartledge, J. E. & Shackleton, N. J. *Paleoceanography* (submitted).

ACKNOWLEDGEMENTS. We thank A. K. Behrensmeier, J. Quade and S. L. Wing for advice and assistance, R. M. Corfield for data from site 577, and T. E. Cerling, M. L. Fogel, J. A. Silfer, E. Thomas, D. J. Velinsky and S. L. Wing for comments. The Smithsonian Institution, the Carnegie Institution of Washington, and NSF funded this project.

## Stability of high-density clinoenstatite at upper-mantle pressures

R. J. Angel\*, A. Chopelas† & N. L. Ross\*

\* Department of Geological Sciences, University College London, Gower Street, London WC1E 6BT, UK  
† Max Planck Institut für Chemie, 6500 Mainz, Germany

SILICATE pyroxenes are major components in mineralogical models of the Earth's upper mantle<sup>1,2</sup>, with the transformation of chain-silicate pyroxenes to denser garnet structures being a possible cause<sup>3</sup> of the seismic discontinuity at 400 km depth that divides the upper mantle from the transition zone. At shallower depths assemblages containing two pyroxenes are stable: calcium and sodium components are accommodated in a diopside-jadeite solid solution<sup>3</sup>, while magnesium and iron form a second, calcium-poor pyroxene. In the absence of experimental data, orthoenstatite was long believed to be the stable polymorph of (Mg, Fe)-pyroxene over the entire upper mantle. More recently, however, petrological experiments<sup>4,5</sup> at pressures and temperatures in excess of 8 GPa and 900 °C have provided evidence for the transformation of Mg-orthopyroxene to a clinopyroxene phase. The thermodynamic and physical properties of this phase are completely unknown. Here we report the results of a high-pressure single-crystal diffraction study which confirm the stability of a high-clinopyroxene phase of  $\text{MgSiO}_3$  at high pressures, and allow an initial estimate to be made of the density changes associated with the transformation of the orthopyroxene component in the Earth's upper mantle.

All of the structures of the pyroxene polymorphs of  $\text{MgSiO}_3$  are based on single chains of corner-sharing tetrahedra which cross-link, by sharing oxygen atoms, parallel bands of octahedrally coordinated magnesium atoms (Fig. 1). The various polymorphs differ in the conformations of the silicate chains and in the relative positions of successive layers of octahedral strips. The stable phase of  $\text{MgSiO}_3$  at ambient pressure and temperature is low clinoenstatite, with orthoenstatite becoming

Received 10 February; accepted 20 May 1992.

- Kennett, J. P. & Stott, L. D. *Nature* **353**, 225–229 (1991).
- Cerling, T. E. *Am. J. Sci.* **291**, 377–400 (1991).
- Aubry, M.-P. *et al. Paleoceanography* **3**, 707–742 (1988).